Flow Turbulence Combust (2013) 91:319–346
DOI 10.1007/s10494-013-9463-y

Numerical Simulation with an Extinction Database for Use with the Eddy Dissipation Concept for Turbulent Combustion

Bjørn Lilleberg · Dominik Christ · Ivar S. Ertesvåg · Kjell Erik Rian · Reinhold Kneer

Received: 9 December 2011 / Accepted: 29 April 2013 / Published online: 28 May 2013

Abstract A Local Extinction approach for treating chemical reaction kinetics within the Eddy Dissipation Concept (EDC) has been examined. It applies a database of pre-calculated chemical time scales, which contains the influence of chemical kinetics that is otherwise time-consuming to calculate. The approach was evaluated against experimental data for two piloted diffusion flames (Sandia/TNF Flame D and Flame E) and a piloted lean-premixed jet burner (PPJB). Results were also compared to the EDC with Fast Chemistry and with full Detailed Chemistry (GRI-Mech 3.0). All validation simulations were carried out using a standard $k-\varepsilon$ turbulence model and the open-source CFD-toolbox OpenFOAM. The Local Extinction approach showed significantly better results than the Fast Chemistry approach while having a comparably small computational cost. For Flame D and the PPJB, the reactions along centerline and in the mixing layer near the nozzle, the reactions were reduced. For Flame E, the Local Extinciton model predicted some lift off of the

B. Lilleberg (✉) · I. S. Ertesvåg
Department of Energy and Process Engineering, Norwegian University of Science and Technology, 7491 Trondheim, Norway
e-mail: lilleber@alumni.ntnu.no

I. S. Ertesvåg
e-mail: Ivar.S.Ertesvag@ntnu.no

D. Christ · R. Kneer
Institute of Heat and Mass Transfer (WSA), RWTH Aachen University, 52056 Aachen, Germany

D. Christ
e-mail: Dominik.Christ@rwth-aachen.de

K. E. Rian
Computational Industry Technologies AS (ComputIT), 7462 Trondheim, Norway

flame. The Detailed Chemistry approach gave the best predictions compared to the experimental data, however the calculation effort was orders of magnitude higher.

Keywords Computational · Modeling · Combustion · Local extinction · Eddy Dissipation Concept · Detailed chemical kinetics · Perfectly Stirred Reactor (PSR)

1 Introduction/Motivation

This paper examines the possibility of explicit coupling of information from detailed chemistry mechanisms to the Eddy Dissipation Concept (EDC) [27, 28] for turbulence-chemistry interaction modeling in Computational Fluid Dynamics (CFD). The EDC has been successfully applied to the numerical simulation of combustion for a longer period of time [13, 14, 28, 29, 33], and it is implemented in most commercial CFD codes available. Today, various approaches to couple chemical kinetics with the EDC exist, which vary in their degree of complexity, detail and computational costs. These approaches range from the fast chemistry assumption ("mixed is burned") involving the solution of Partial Differential Equations (PDE) for the major species, to solving PDEs and systems of Ordinary Differential Equations (ODE) (describing Perfectly Stirred Reactors) for each species of a detailed chemical mechanism. An alternative approach uses datasets that state when local extinction of the flame occurs. These datasets are determined a priori and can therefore be used in the simulation of turbulent combustion at a low computational cost. This approach has been previously demonstrated by Byggstøyl and Magnussen [5] and Gran et al. [15] using one-step global reaction mechanisms. In this study the local extinction data were determined on the basis of a detailed chemical mechanism and demonstrated the applicability of the EDC model with the Local Extinction approach to both diffusion and premixed flames. Furthermore, comparisons with full detailed chemistry calculations are presented which allow for an effective assessment of the Local Extinction approach quality. The Local Extinction approach makes it possible to include effects of finite-rate chemistry in a computationally very fast manner. This is favorable for doing Large Eddy Simulations (LES) where transient computation is necessary and the number of grid cells is particularly large due to a fine resolution of the flow and a full three-dimensional computational grid. Another area of application is industry-scale simulations. In these types of problems, the computational domains are often much bigger (containing more grid cells) than in experimental burners used to validate combustion models. This makes simulations with detailed chemistry very time consuming and hence, a computationally inexpensive treatment of the chemical kinetics is sought. This study intends to provide a validated basis for these applications.

In this work the standard $k-\varepsilon$ model was used to simulate the Sandia/TNF Flames D and E (although with main focus on Flame D) [2], which are partially-premixed piloted methane-air jet flames, and a Piloted Premixed Jet Burner (PPJB) [9, 10]. The Flame D setup has been used as a validation case for a number of simulations with various models [1, 17, 20, 22, 31, 44], including EDC, Probability Density Functions (PDF), Conditional Moment Closure (CMC) models and various types of flamelet models. Flame E has been simulated with models based on PDF

transport (e.g. [41, 42]) and CMC (e.g. [23]). It seems, however, that it has not been simulated with simple statistical models like the EDC or flamelet models, combined with a $k-\varepsilon$ model, in the archival literature.

In the study of Zahirović et al. [44], Reynolds-Averaged Navier–Stokes (RANS) simulations of the Sandia Flame D, using the EDC for modeling the turbulence-chemistry interaction, with a detailed description of the chemistry, was reported. The chemical mechanism ARM19 was used, and turbulence was modeled with a standard $k-\varepsilon$ model, a realizable $k-\varepsilon$ model and a Reynolds Stress Equation (RSE) model. In the standard $k-\varepsilon$ model, the model constant $C_{\varepsilon 1}$ was changed from 1.44 (the standard value) to 1.60. The authors reported that the realizable $k-\varepsilon$ model and the RSE model shifted the temperature peak towards the burner. The tuning of the standard $k-\varepsilon$ model constant yielded a better prediction of the temperature slope (axial plot) up to its peak. The EDC predicted, overall, slightly too high peak temperatures. However, the tuning of the model constant led to a considerable decrease of the turbulent kinetic energy. They also showed that the CO peaks predicted with the EDC were only slightly higher than the measurements. Whereas the realizable $k-\varepsilon$ model and Reynolds stress model predicted OH in good agreement with the measurements, the tuned standard $k-\varepsilon$ model gave a distinct overestimation of the radical. No radial plots of scalars were reported in their work. Kim et al. [22] reported the usage of a standard $k-\varepsilon$ model, with the EDC to account for the turbulence-chemistry interaction, for the Sandia Flame D. In their work various simplified reaction mechanisms were employed to account for detailed chemistry. All the mechanisms overpredicted temperature, but some of the simplified mechanisms were shown to give fairly good predictions of CO and H_2 compared to measurements. Other investigators of Flame D, Merci and Dick [31] and Amani and Nobari [1], choose a reduced $C_{\varepsilon 2}$ (to 1.80) to achieve the same effects, while Habibi et al. [17] choose a weaker modification by using $C_{\varepsilon 1} = 1.50$. Merci and Dick [31] found that the numerical discretization scheme was important for the spreading of the jet and the results showed that the combustion model and kinetics model also have effects on spreading and mixing. The choice of turbulence-model constants appears to be a choice of where in the flame the turbulent mixing should be appropriate.

The standard values of the $k-\varepsilon$ model, from Launder and Spalding [24], result in an overprediction of spreading and turbulence diffusion of round jet flows. This tends to increase downstream from the nozzle. The overpredicted mixing also exagerates the fuel conversion and hence, affects the location of heat release and the development of the density and velocity fields. To reduce the spreading/diffusion, various modifications have been suggested (in [24] and later by others). The main approach has been to increase $C_{\varepsilon 1}$ or reduce $C_{\varepsilon 2}$, as seen in the literature referred above. It is known (see [16, 33]) that the turbulence modeling can have considerable effects on the combustion results. Hence, for combustion-model investigations (although not in general) it will be appropriate to make "ad hoc" modifications of the turbulence models to give the best representation of the turbulent flow field.

The PPJB is intended to become a validation case for computational modeling of premixed turbulent combustion, and some numerical computations of the PPJB have recently been reported by Dunn et al. [11] and Rowinski and Pope [36]. Dunn et al. [11] reported that the predictive capabilities of the RANS turbulence models were regarded as the major contributor to mismatch between predictions and experimental data. According to Rowinski and Pope [36], a revised micro-

mixing model was needed for the joint velocity-turbulence frequency-composition PDF method. Measurements of mean and Root Mean Square (RMS) velocity, as well as scalar data, are available for both Flame D [2, 3, 37] and PPJB [9, 10]. In the present work the EDC for turbulence-chemistry interaction, with three different chemistry-modeling approaches, has been implemented in the open source CFD toolbox OpenFOAM [34].

The paper is divided into three main parts. The first part of the paper describes the mathematical modeling, and the second part describes details about the implementation of the model variants. Finally, the computational results from the three model variants are compared to experimental data for the burners, results are discussed, and conclusions are drawn.

2 Mathematical Modeling

The open source CFD-toolbox OpenFOAM [34] has been used in this work and the Eddy Dissipation Concept (EDC) for turbulence-chemistry interaction, as described by Magnussen [27] and Gran and Magnussen [14], has been specially implemented for the study of the three chemistry-modeling approaches.

2.1 Governing equations

The Favre-averaged equations for transient compressible flow when using the standard $k-\varepsilon$ model [24] are as follows:
Overall mass conservation:

$$\frac{\partial \bar{\rho}}{\partial t} + \frac{\partial}{\partial x_j}\left(\bar{\rho}\widetilde{u}_j\right) = 0 \tag{1}$$

where ρ is the density and u_j the Cartesian velocity component in the x_j-direction, the overbar denotes the ordinary (Reynolds) average, while the tilde denotes mass-weighted (Favre) averages.

Conservation of mean momentum:

$$\frac{\partial}{\partial t}\left(\bar{\rho}\widetilde{u}_i\right) + \frac{\partial}{\partial x_j}\left(\bar{\rho}\widetilde{u}_i\widetilde{u}_j\right) = -\frac{\partial \bar{p}}{\partial x_i} + \frac{\partial}{\partial x_j}\left(\bar{\tau}_{ij} - \bar{\rho}\widetilde{u_i''u_j''}\right) + \bar{\rho}\widetilde{f}_i \tag{2}$$

where p is pressure, τ_{ij} is the viscous stress tensor and f_i is the body-force acceleration in the x_i-direction.

Transport equation for the mean mass fraction of an individual species Y_k in a mixture of N species:

$$\frac{\partial}{\partial t}\left(\bar{\rho}\widetilde{Y}_k\right) + \frac{\partial}{\partial x_j}\left(\bar{\rho}\widetilde{Y}_k\widetilde{u}_j\right) = \frac{\partial}{\partial x_j}\left(\bar{\rho}D\frac{\partial \widetilde{Y}_k}{\partial x_j}\right) - \frac{\partial}{\partial x_j}\left(\bar{\rho}\widetilde{u_j''Y_k''}\right) + \overline{\omega_k}, \quad k = 1, \ldots, N_{\text{species}} \tag{3}$$

where D is the mass diffusion coefficient, ω_k is the volumetric net rate of production of species k due to chemical reactions and N_{species} is the number of species considered.

The energy transport equation formulated in terms of total enthalpy h:

$$\frac{\partial}{\partial t}\left(\bar{\rho}\widetilde{h}\right)+\frac{\partial}{\partial x_j}\left(\bar{\rho}\widetilde{h}\widetilde{u}_j\right)=\frac{\partial}{\partial x_j}\left(\bar{\rho}\alpha\frac{\partial\widetilde{h}}{\partial x_j}-\bar{\rho}\widetilde{u_j''h''}\right)+\overline{S_h} \tag{4}$$

where α is the thermal diffusivity and S_h is internal production of thermal energy.

The Reynolds stresses are modeled as:

$$\bar{\rho}\widetilde{u_i''u_j''}=-\mu_{\mathrm{t}}\left(\frac{\partial\widetilde{u}_i}{\partial x_j}+\frac{\partial\widetilde{u}_j}{\partial x_i}-\frac{2}{3}\delta_{ij}\frac{\partial\widetilde{u}_k}{\partial x_k}\right)+\frac{2}{3}\bar{\rho}\widetilde{k}\delta_{ij} \tag{5}$$

where δ_{ij} is the Kronecker delta, $\mu_{\mathrm{t}}=C_\mu\bar{\rho}\widetilde{k}^2/\widetilde{\varepsilon}$ is the eddy viscosity, and C_μ is a model constant.

Gradient model for the turbulence fluxes in Eqs. 3 and 4:

$$-\bar{\rho}\widetilde{u_i''Y_k''}=\frac{\mu_{\mathrm{t}}}{\sigma_{\mathrm{t}}}\frac{\partial\widetilde{Y}_k}{\partial x_i} \tag{6}$$

$$-\bar{\rho}\widetilde{u_i''h''}=\frac{\mu_{\mathrm{t}}}{\sigma_{\mathrm{t}}}\frac{\partial\widetilde{h}}{\partial x_i} \tag{7}$$

where σ_{t} is a model constant.

The equation for turbulence kinetic energy k:

$$\frac{\partial}{\partial t}\left(\bar{\rho}\widetilde{k}\right)+\frac{\partial}{\partial x_i}\left(\bar{\rho}\widetilde{u}_i\widetilde{k}\right)=\frac{\partial}{\partial x_i}\left[\left(\mu+\frac{\mu_{\mathrm{t}}}{\sigma_k}\right)\frac{\partial\widetilde{k}}{\partial x_i}\right]+G-\bar{\rho}\widetilde{\varepsilon} \tag{8}$$

and the equation for dissipation rate of turbulence kinetic energy ε:

$$\frac{\partial}{\partial t}\left(\bar{\rho}\widetilde{\varepsilon}\right)+\frac{\partial}{\partial x_i}\left(\bar{\rho}\widetilde{u}_i\widetilde{\varepsilon}\right)=\frac{\partial}{\partial x_i}\left[\left(\mu+\frac{\mu_{\mathrm{t}}}{\sigma_\varepsilon}\right)\frac{\partial\widetilde{\varepsilon}}{\partial x_i}\right]+C_{\varepsilon1}\frac{\widetilde{\varepsilon}}{\widetilde{k}}G-C_{\varepsilon2}\bar{\rho}\frac{\widetilde{\varepsilon}^2}{\widetilde{k}} \tag{9}$$

where σ_k, σ_ε, $C_{\varepsilon1}$ and $C_{\varepsilon2}$ are model constants, and the rate of turbulence kinetic energy production G is given as

$$G=-\bar{\rho}\widetilde{u_i''u_j''}\frac{\partial\widetilde{u}_i}{\partial x_j} \tag{10}$$

Recommended values for the model constants are given by [21, 24] as $C_\mu=0.09$, $C_{\varepsilon1}=1.44$, $C_{\varepsilon2}=1.92$, $\sigma_k=1.0$, $\sigma_\varepsilon=1.3$ and $\sigma_{\mathrm{t}}=0.7$.

2.2 The EDC for turbulent combustion

The Eddy Dissipation Concept (EDC), originally presented by Magnussen and Hjertager [28], has been developed by B. F. Magnussen and co-workers at the Norwegian University of Science and Technology (NTNU) over four decades [12, 14, 26, 27, 35]. EDC gives an expression for the mean reaction rate, cf. Eq. 3. The model assumes that chemical reactions occur where the dissipation of turbulence energy takes place, that is, in the *fine structures*, which have characteristic dimensions that are of the order of the Kolmogorov scales. These structures are not evenly distributed in time and space but are concentrated in certain regions (*fine-structure regions*) that occupy a fraction of the flow. In the model expressions below, different superscripts

refer to states within fine structures (*), surroundings (°), and mean values of the computational cell (~).

The ratio of the mass of the *fine structure regions* to the total mass is expressed as

$$\gamma = \left(\frac{3C_{\mathrm{D2}}}{4C_{\mathrm{D1}}^2}\right)^{1/4} \left(\frac{\nu^* \widetilde{\varepsilon}}{\widetilde{k}^2}\right)^{1/4} \tag{11}$$

where the model constants are $C_{\mathrm{D1}} = 0.134$ and $C_{\mathrm{D2}} = 0.50$ [12, 27] and ν^* is the kinematic viscosity of the fine-structure mixture. The ratio of the mass of the fine structures to the total mass is modeled as $\gamma^* = \gamma^3$.

The rate at which mass is transferred between the fine structures and the surroundings is estimated as

$$\dot{m}^* = \left(\frac{3}{C_{\mathrm{D2}}}\right)^{1/2} \left(\frac{\widetilde{\varepsilon}}{\nu^*}\right)^{1/2} \tag{12}$$

Hence, the residence time in the fine structure homogeneous reactor is given as: $\tau^* = 1/\dot{m}^*$. The expressions for γ, γ^* and $\dot{m}^*$ follows from the cascade model, which models the energy transfer from large to smaller scales.

The mass-averaged mean reaction rate according to the EDC can be given [27] as

$$-\overline{\omega_k} = \frac{\bar{\rho}\gamma^2 \dot{m}^* \chi}{1 - \gamma^* \chi} \left(\widetilde{Y}_k - Y_k^*\right), \quad k = 1, \ldots, N_{\mathrm{species}} \tag{13}$$

and the relationship between the mass-averaged mean state, fine-structure state and surrounding state is expressed as

$$\widetilde{\Psi} = \gamma^* \chi \Psi^* + \left(1 - \gamma^* \chi\right) \Psi^\circ \tag{14}$$

Here, χ is the reacting fraction of the fine structures, which depends on three aspects: probability of coexistence of the reactants, degree of heating and a limiter to the reaction due to lack of reactants. Further details on χ are explained in the section on fast chemistry. The reaction rate further depends on the mean mass fraction $\widetilde{Y}_k$ for species k and the mass fractions inside the fine structures Y_k^*. The former values are known from solving the transport equations for individual mass fractions, Eq. 3. The fine-structure mass fractions Y_k^* must be computed, and three possible approaches of calculating them are presented below.

2.3 The EDC Fast Chemistry approach

If it can be assumed that there is sufficient residence time in the fine structures, the fast chemistry limit is obtained. It is further assumed that the combustion can be represented by the single irreversible one-step reaction

$$1 \text{ kg Fuel (F)} + r_{\mathrm{F}} \text{ kg Oxidizer (O)} \rightarrow (1 + r_{\mathrm{F}}) \text{ kg Products (P)} \tag{15}$$

with the stoichiometric oxidizer-air ratio r_{F} (mass based). Written in a more general form

$$\nu_{\mathrm{R1}} \frac{M_{\mathrm{R1}}}{\widetilde{M}} \left[\frac{\mathrm{kg_{R1}}}{\mathrm{kg_{total}}}\right] \text{Reactant 1 (R1)} + \ldots \rightarrow \nu_{\mathrm{P1}} \frac{M_{\mathrm{P1}}}{\widetilde{M}} \left[\frac{\mathrm{kg_{P1}}}{\mathrm{kg_{total}}}\right] \text{Product 1 (P1)} + \ldots \tag{16}$$

with corresponding stoichiometric coefficients ν_i, molar masses M_i and the mean molar mass $\widetilde{M}$ of the computational cell, it is possible to define a set of scaled mass fractions, extending the approach that is described by Gran [13] and Gran and Magnussen [14] with

$$\hat{Y}_k = \frac{\widetilde{Y}_k}{\nu_k \frac{M_k}{\widetilde{M}}} \tag{17}$$

Changes in the scaled mass fractions correspond to stoichiometrically proportional changes in the unscaled mass fractions.

The Fast Chemistry approach assumes that the reaction converts as many reactants as stoichiometrically possible, i.e. the amount of converted reactants is limited in a rich mixture by the oxidizer available and in a lean mixture by the fuel available [27, 28]. Using scaled mass fractions of reactants, the scarce component can be obtained trivially as

$$\hat{Y}_{\min} = \min\left[\hat{Y}_{\mathrm{F}}, \hat{Y}_{\mathrm{O}}\right]. \tag{18}$$

The composition of reactants R_i and products P_i, corresponding to complete combustion ("cc"), can thus be obtained as

$$\hat{Y}_{\mathrm{R},k,\mathrm{cc}} = \hat{Y}_{\mathrm{R},k} - \hat{Y}_{\min} \tag{19}$$

$$\hat{Y}_{\mathrm{P},k,\mathrm{cc}} = \hat{Y}_{\mathrm{P},k} + \hat{Y}_{\min} \tag{20}$$

Then, the fine structure composition can be obtained from the mass fractions at complete combustion in Eqs. 19 and 20 by re-scaling:

$$Y_k^* = \hat{Y}_{k,\mathrm{cc}} \cdot \nu_k \frac{M_k}{\widetilde{M}} \tag{21}$$

Using the extended approach it is also possible to use more than one global reaction, e.g. including the formation of CO [8],

$$\mathrm{CH_4} + 1.5\mathrm{O_2} \rightarrow \mathrm{CO} + 2\mathrm{H_2O} \tag{22}$$

$$\mathrm{CO} + 0.5\mathrm{O_2} \rightarrow \mathrm{CO_2} \tag{23}$$

For multiple reactions, it becomes necessary to define a priority of fuels. If oxygen is the scarce reactant, the fuel with the highest priority is consumed first and if any oxygen is left afterwards, the fuel with the next highest priority can react with the remaining oxygen and so on. For the two-step reaction shown above, methane would be defined as first and carbon monoxide as second priority fuel. The scaling of mass fractions, Eq. 17, has to occur separately for each reaction equation since the reactants and products, as well as their stoichiometric factors, are different. This extension to multiple reactions, however, is only employable up to a small number of chemical reactions as increasing interactions between chemical reactions require a more elaborate modelling.

Furthermore, the EDC defines a function for the reacting fraction of the fine structures χ. This function is defined [14, 27] as

$$\chi = \chi_1 \cdot \chi_2 \cdot \chi_3 \tag{24}$$

where χ_1 is a measure of the coexistence of reactants,

$$\chi_1 = \frac{\left(\hat{Y}_{\min} + \hat{Y}_P\right)^2}{\left(\hat{Y}_F + \hat{Y}_P\right)\left(\hat{Y}_O + \hat{Y}_P\right)} \tag{25}$$

with the summarized scaled mass fraction of products $\hat{Y}_P = \sum_k \hat{Y}_{P,k}$.

χ_2 is an expression denoting that reaction products are present. These are assumed to be hot and are required to ignite the mixture,

$$\chi_2 = \min\left[\frac{\hat{Y}_P}{\gamma\left(\hat{Y}_P + \hat{Y}_{\min}\right)}, 1\right] \tag{26}$$

χ_3 limits the reaction due to lack of reactants,

$$\chi_3 = \min\left[\frac{\gamma\left(\hat{Y}_P + \hat{Y}_{\min}\right)}{\hat{Y}_{\min}}, 1\right]. \tag{27}$$

Here, in case of more than one reaction, the calculation for χ is only performed for the fuel with the highest priority. With the parameters χ and Y_k^* thus determined, the reaction rate can be calculated according to Eq. 13.

2.4 The EDC Detailed Chemistry approach

Finite-rate chemical kinetics are taken into account by treating the fine structures as constant-pressure and adiabatic homogeneous reactors. The fine structure mass fraction values Y_k^* in Eq. 13 can be found by solving a set of Ordinary Differential Equations (ODE) describing a Perfectly Stirred Reactor (PSR) [13, 14],

$$\frac{dh^*}{dt} = 0 \tag{28}$$

$$\frac{dp^*}{dt} = 0 \tag{29}$$

$$\frac{dY_k^*}{dt} = \frac{\omega_k^*}{\rho^*} + \frac{1}{\tau^*}\left(Y_k^\circ - Y_k^*\right), \quad k = 1, \ldots, N_{\text{species}} \tag{30}$$

The reaction rate ω_k^* is evaluated from a chemical kinetics mechanism and Y_k° is the mass fraction of the inflow to the reactor. It is assumed [14, 27] that the reactors are at steady state, and the steady-state solution of Eqs. 28–30 is usually achieved by integrating the equations in time to steady state. When simulating finite-rate chemistry, the value for the reacting fine structure fraction χ in Eq. 13 is set to unity [13, 14].

2.5 The EDC Local Extinction approach

An approach for modeling local extinction in reacting turbulent flows was proposed by Byggstøyl and Magnussen [5] and Gran et al. [15]. This model was based on EDC and the extinction was assumed to take place in the turbulent fine structures. The

characteristic time scale for the turbulent fine structures is expressed as from Eq. 12, $\tau^* = 1/\dot{m}^*$.

To determine whether local extinction takes place in the fine structures, this time scale was compared to a chemical time scale τ_{ch}. If the turbulent fine structures are treated as PSRs, a set of PSR calculations can be performed to establish a diagram for τ_{ch} for different inlet temperatures and equivalence ratios. The model predicts extinction if $\tau^\star < \tau_{ch}$ and the reaction rate $\overline{\omega_k}$ (Eq. 13) is set to zero if the condition is fulfilled. Otherwise, the reaction rate is determined with the Fast Chemistry approach. In this way, the Local Extinction approach slows down or prevent the reactions compared to the Fast Chemistry approach.

3 Numerical Modeling

In this study the chemical kinetic mechanism GRI-Mech 3.0 [40] was used for both EDC with Detailed Chemistry and for EDC with Local Extinction. This mechanism has been specially designed for combustion of natural gas with air and is, hence, well suited for simulations of methane-air combustion. The mechanism comprises 325 elementary reactions with 53 species ($N_{species}$ in Eqs. 3, 13 and 30).

In both the Local Extinction and Detailed Chemistry approaches, Eq. 30 was integrated in time. Assuming adiabatic and isobaric reactors, Eqs. 28 and 29 were not included in the calculations. This set of ODEs is numerically very stiff [25], and for this reason the robust RADAU5 algorithm [18, 19] was used here.

3.1 Time scale for Local Extinction

To use the Local Extinction approach it is necessary to pre-calculate a database of chemical time scales for different inlet temperatures and equivalence ratios. This was done by performing a PSR calculation for each set of inlet temperature and equivalence ratio.

The method for finding the chemical time scales was as follows: Initially, the inlet temperature and the mixture equivalence ratio were set. Equation 30 was then integrated in time while increasing the inlet temperature to ignite the mixture. After ignition had taken place, the inlet temperature was set back to its starting value and if the temperature did not drop off, the PSR could maintain combustion. Initially, for the ignition of the mixture, the PSR residence time τ^* was set to 1 s. If the PSR could maintain combustion, the value for τ^* was gradually reduced in a coarse way to find the approximate time scale for extinction. When the approximate time scale had been found, the procedure was repeated to find the final, and more precise, value for the lowest τ^* just before extinction occurred. Figure 1 shows the chemical time scales τ_{ch} for methane and air at different inlet temperatures and equivalence ratios. The step-like nature is due to a logarithmic timestepping in determining the chemical time scale, τ_{ch}.

3.2 Testing for chemical time scale and flammability limits

While the pre-calculated database of chemical time scales could be used directly to test for local extinction at given PSR inlet temperature and equivalence ratio, it was

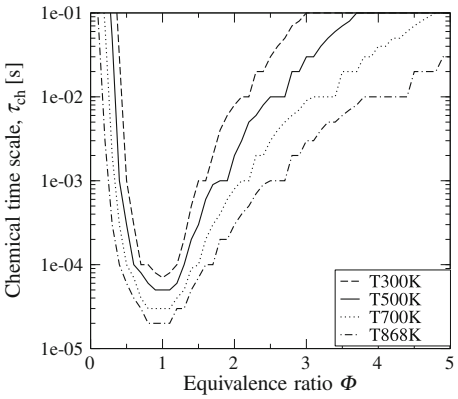

Fig. 1 Calculated chemical time scales τ_{ch} for different inlet temperatures and equivalence ratios. Mixture of methane and air

found that it was feasible to further reduce the datasets before applying them to turbulence-chemistry interaction modeling. From each curve, a minimal chemical time scale could be extracted. According to this method, local extinction occurs when $\tau^* < \tau_{ch,min}$. While it would be also possible to further determine upper and lower flammability limits from Fig. 1, this showed no practical improvement in this investigation and on rare occasions even led to numerical instabilities. If testing for PSR inlet temperatures that had no corresponding dataset present in the database, the values of $\tau_{ch,min}$ were linearly interpolated between the two closest datasets. If the PSR inlet temperature was above the autoignition temperature of the fuel, no local extinction was assumed to occur.

3.3 Application to CFD simulation of gaseous combustion

In order to assess the performance of both the Local Extinction approach and the Local Extinction database for methane, two reference methane-air flames (explained in detail below) were simulated using OpenFOAM [34]. Discretization of the convective term of all transport equations was performed with the Linear Upwind interpolation, which has second-order accuracy and is described, for example, by Waterson and Deconinck [43]. The calculations were performed using steady RANS equations. Due to the strong coupling of species mass fractions with the energy equation and thus the density, it was necessary to use considerable under-relaxation on the species transport equations. Furthermore, the flow was initialized with a cold, non-reacting CFD solution. When applying the Detailed Chemistry approach, the EDC is very sensitive to initial conditions with respect to stability. Therefore, the Detailed Chemistry approach used the converged Local Extinction solution as starting value. The kinetic data for one-step and two-step combustion were taken from Dryer and Glassman [8].

The computational time to reach convergence for the considered cases using the Fast Chemistry and Local Extinction approach was in the range of minutes on a single node state-of-the-art personal computer. With the Detailed Chemistry approach, the time to reach a convergent solution was a few days to a week depending on the flow rates, the grid resolution and how detailed the chemical reaction mechanism was. No noticeable differences in computational time between the Fast Chemistry

and Local Extinction approaches were observed. Grid refinement studies conducted with the Fast Chemistry or Local Extinction approaches were applied to evaluate grid convergence. The numerical grids which showed grid convergence for the computationally fast approaches were applied in the detailed chemistry calculations.

3.4 Sandia Flames D and E

Flames D and E from the Sandia/TNF workshop [2, 3] are piloted methane-air diffusion flames with an axi-symmetric geometry. In this study, the main focus was on numerical simulations of Flame D.

The central main jet consisted of a methane-air mixture with 25 vol-% CH_4 corresponding to an equivalence ratio of 3.17. This is above the upper flammability limit of methane so combustion is still controlled by mixing. It was surrounded by a pilot flame and a slow coflow of air outside. The bulk velocities of the main jet were 49.6 m/s (Flame D) and 74.4 m/s (Flame E), the pilot 11.4 m/s (Flame D) and 17.1 m/s (Flame E), and the coflow 0.9 m/s. The main jet nozzle had an inner diameter (D) of 7.2 mm, which resulted in a jet Reynolds number of 22400 (Flame D). Flame D exhibited local extinction to a limited degree, while Flame E had more local extinction, cf. Barlow and Frank [2]. The pilot flame was burning a mixture of C_2H_2, H_2, air, CO_2, and N_2 with an enthalpy and equilibrium composition that is equivalent to a mixture of methane and air at an equivalence ratio of $\Phi = 0.77$. The energy release by the pilot amounted to about 6% of the main jet flame with a gas temperature of 1880 K. More details, including sketches of the burner, are given by Barlow and Frank [2] and Barlow et al. [3].

The CFD simulations of Flame D were conducted on an axi-symmetric numerical mesh. Simulations of both jet and pilot pre-inlet pipes were conducted beforehand in order to obtain fully-developed profiles of velocity as well as turbulence kinetic energy and dissipation, and these were used as inlet values for the Flame D computations. The computational domain extended $20.5D$ in the radial direction and $76.4D$ in the axial direction, and the mesh was comparatively coarse consisting of 111×41 cells in the axial and radial direction, respectively. The jet pipe was resolved with 4 cells, and the pilot was resolved with 5 cells, in the radial direction. However, a mesh refinement study showed no improvement in the considered target quantities: temperature and species concentrations. For the Flame E simulations the computational domain extended $20.5D$ in the radial direction and $138D$ in the axial direction. The mesh consisted of 100×50 cells in the axial and radial direction, respectively. The jet pipe was resolved with 8 cells, and the pilot was resolved with 10 cells, in the radial direction. Bulk profiles were applied at the inlet boundaries. Also for the Flame E, a mesh refinement study showed no improvement in the considered target quantities.

Standard wall-functions were used along the walls of the domain when relevant. Heat transfer by radiation was modeled using the P1 model described by Siegel and Howell [38]; the absorption and emission coefficients for the gas mixture were calculated using a custom implementation of the weighted-sum-of-grey-gases model with the model coefficients from Smith et al. [39].

The mixture fraction is defined according to Barlow and Frank [2] as

$$\widetilde{\xi} = \frac{2\left(\widetilde{Y}_{\mathrm{C}} - Y_{\mathrm{C,coflow}}\right)/M_{\mathrm{C}} + \left(\widetilde{Y}_{\mathrm{H}} - Y_{\mathrm{H,coflow}}\right)/2M_{\mathrm{H}}}{2\left(Y_{\mathrm{C,main}} - Y_{\mathrm{C,coflow}}\right)/M_{\mathrm{C}} + \left(Y_{\mathrm{H,main}} - Y_{\mathrm{H,coflow}}\right)/2M_{\mathrm{H}}} \tag{31}$$

with the elemental mass fractions of carbon $\widetilde{Y}_C$ and hydrogen $\widetilde{Y}_H$ and the atomic weights of carbon M_C and hydrogen M_H, respectively. The mass fractions of carbon and hydrogen at the coflow inlet (air) were zero. At the main jet inlet, the bulk mass fractions of carbon and hydrogen were $Y_{\mathrm{C,main}} = 0.1170$ and $Y_{\mathrm{H,main}} = 0.0393$, respectively.

3.5 Piloted Premixed Jet Burner

The Piloted Premixed Jet Burner (PPJB) [9] consisted of a small diameter ($D = 4$ mm) lean premixed jet (CH_4 and air, $\Phi = 0.5$, $T = 300$ K) piloted by a low-velocity pilot (stoichiometric CH_4 and air, $T = 2280$ K, $U_{\mathrm{bulk}} = 5.3$ m/s) and surrounded by a large diameter hydrogen-air combusting coflow ($\Phi = 0.43$, $T = 1500$ K, $U_{\mathrm{bulk}} = 4.0$ m/s). Both the pilot and coflow were taken to be in chemical equilibrium [9]. Four jet velocities have been experimentally investigated. In this study the 50 m/s jet with a Reynolds number 12500 was simulated. The geometry of the burner is axi-symmetric. More details, including sketches of the burner, can be found in Dunn et al. [9, 10].

The computational grid used in the present calculations was axi-symmetric, non-uniform and rectilinear. The transverse grid was chosen so that the grid lines coincided with the fixed geometric points defined by the jet, pilot and coflow, and with the grid lines concentrated in the region around the high velocity jet exit. The grid had its origin corresponding to the center of the central jet at the exit plane, and the domain extended $30D$ in the radial direction and $125D$ in the axial direction. At the inflow boundaries, the respective bulk velocities were set for the jet, pilot and coflow. The values for k and ε were calculated for a turbulence intensity taken as 5 %, and the turbulence length scale was estimated as 10 % of the inlet widths (hydraulic diameters). For all of the inflow boundaries, a zero gradient pressure boundary was applied. The boundary along the axial direction at $r/D = 30$ was taken to be a perfect-slip wall, and the outflow boundary had a uniform total pressure equal to one atmosphere and zero gradient for all other fields. In the standard $k - \varepsilon$ turbulence model, the constant $C_{\varepsilon 1}$ was modified from 1.44 to 1.60 [7, 30]. Initial simulations were conducted in order to asses the influence of $C_{\varepsilon 1}$ on the results. Initial tests showed that the best agreement between simulation results and experimental data was observed for $C_{\varepsilon 1} = 1.60$. The model constant $C_{\varepsilon 1} = 1.44$ gave more spreading of the jet. Generally, adjusting the value $C_{\varepsilon 1}$ from 1.44 to 1.60 improved the mean velocity field, but at the expense of decreased predictive capabilities for the RMS velocity fields.

The accuracy of the spatial discretization was investigated with four different grids, two coarse: 150×100, 250×100; two fine: 300×165 and 500×165 (axial $\times$ radial number of nodes). All grids were non-uniform and rectilinear, and with the grid lines concentrated in the region around the high-velocity jet exit. In the coarse grids the jet pipe was resolved with 4 cells in the radial direction, and in the fine grids 8 cells were used. The differences between the four solutions were very small, and it was therefore concluded that the 150×100 grid was sufficiently accurate for testing the mathematical models on the piloted premixed jet burner.

Heat transfer by radiation was neglected for the PPJB.

The mixture fractions for the jet and coflow, $\widetilde{\xi}_{\text{jet}}$ and $\widetilde{\xi}_{\text{coflow}}$, respectively, are given by Barlow et al. [4] as

$$\widetilde{\xi}_{\text{jet}} = \frac{\widetilde{Y}_{\text{C}} \left(Y_{\text{H,coflow}} - Y_{\text{H,pilot}}\right) + Y_{\text{C,pilot}} \left(\widetilde{Y}_{\text{H}} - Y_{\text{H,coflow}}\right)}{Y_{\text{C,jet}} \left(Y_{\text{H,coflow}} - Y_{\text{H,pilot}}\right) + Y_{\text{C,pilot}} \left(Y_{\text{H,jet}} - Y_{\text{H,coflow}}\right)} \tag{32}$$

$$\widetilde{\xi}_{\text{coflow}} = \frac{\widetilde{Y}_{\text{C}} \left(Y_{\text{H,pilot}} - Y_{\text{H,jet}}\right) + Y_{\text{C,jet}} \left(\widetilde{Y}_{\text{H}} - Y_{\text{H,pilot}}\right) + Y_{\text{C,pilot}} \left(Y_{\text{H,jet}} - \widetilde{Y}_{\text{H}}\right)}{Y_{\text{C,jet}} \left(Y_{\text{H,coflow}} - Y_{\text{H,pilot}}\right) + Y_{\text{C,pilot}} \left(Y_{\text{H,jet}} - Y_{\text{H,coflow}}\right)} \tag{33}$$

4 Results

4.1 Sandia Flame D and E

Simulation results were compared to experimental data from Barlow and Frank [2] and Schneider et al. [37]. A description of the most important characteristics for Flame D is given in the following. The radial profiles of the mean velocity showed generally a good agreement between predictions and experimental data. At $x/D = 7.5$ and $x/D = 15$ ($D = 7.2$ mm), the calculated velocities were slightly higher on the outside of the central jet compared to the experimental data. Similar effects could be observed for the RMS velocities, except for the radial profile at $x/D = 45$ where the predicted values were noticeably smaller than those measured. The profiles of the mean mixture fractions, Fig. 2, and the mean and RMS velocities showed generally some too high values in the mixing layer of the first part of the jet flame. This indicated underpredicted turbulent mixing in the zone near the nozzle. Then, from a location between $x/D = 15$ and $x/D = 30$, the spreading was overpredicted leading to lower maximum values and wider profiles for the mentioned quantities, e.g. for the mean mixture fraction shown in Fig. 2d. This development went on and was increased further downstream compared with the experimental data. The tendency of overpredicting spreading was clearly less for Detailed Chemistry compared to Fast Chemistry. Also the Local Extinction approach predicted less spreading compared to Fast Chemistry. The constant $C_{\varepsilon 1}$ in the standard $k - \varepsilon$ turbulence model, was 1.44 for all the presented Flame D simulations. For this case, the standard set of model constants appeared to give the best development of the turbulent flow field.

In general, the Detailed Chemistry approach gave the best predictions compared to the measurements as seen in Figs. 2, 3, 4, 5 and 6. Along the central axis, the peak temperature of all approaches for the EDC agrees well with the experimental data. The temperature profiles, Fig. 3, show the combined effect of the turbulence mixing and the heat release from the chemical reactions. The Fast Chemistry approach led to too early fuel consumption and heat release, while Detailed Chemistry delayed the reactions in accordance with the experimental data. With the one-step reaction, this rise occurs earlier than with the two-step reactions. In Fig. 3, it is seen that the Local Extinction approach had a notable effect on the temperature development compared to Fast Chemistry, although not as strong as the Detailed Chemistry. The immediate conversion of fuel was inhibited close to the nozzle by the Local Extinction approach. This is also seen in Figs. 4–6 for O_2, CO_2 and CO, respectively. The Local Extinction

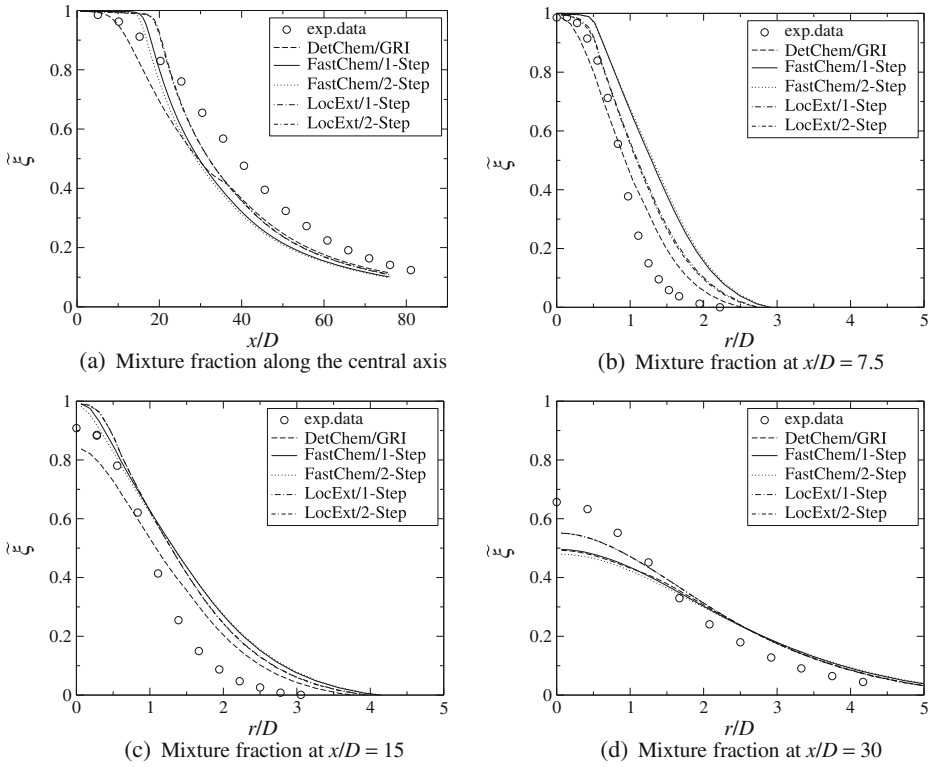

(a) Mixture fraction along the central axis
(b) Mixture fraction at $x/D = 7.5$
(c) Mixture fraction at $x/D = 15$
(d) Mixture fraction at $x/D = 30$

Fig. 2 Mixture-fraction predictions and measurements for the Flame D burner. Experimental data from Barlow and Frank [2] and simulations with the EDC and different approaches for the chemical kinetics. DetChem: Detailed Chemistry approach. FastChem: Fast Chemistry approach. LocExt: Local Extinction approach

approach delayed the reactant consumption compared to Fast Chemistry, reactions were slowed down. From $x/D = 20$ to about $x/D = 40$, the O_2 mass fraction was around zero for Fast Chemistry and Local Extinction. The mass fraction of CO was only considered with the detailed chemical mechanism and the two-step reaction. While the Detailed Chemistry approach resulted in accurate peak values, the two-step reaction with the Fast Chemistry and Local Extinction approach overpredicted the CO mass fractions with the axial profile shifted too close to the burner.

The radial profiles at $x/D = 7.5$ and $x/D = 15$ showed that the Detailed Chemistry approach gave a very good prediction for the peak values of the scalars. However, the profiles were slightly shifted away from the central axis compared to the measurements. The radial profiles of the Fast Chemistry and the Local Extinction approach showed overpredicted temperature peaks which were similar for both the one-step and two-step reaction. The production of CO_2, as well as CO, were also overpredicted by these two approaches. Here, oxygen was consumed entirely in the same way as for the axial profiles.

At $x/D = 30$ the Detailed Chemistry approach overpredicted the reaction rate compared to the measurements. In the predictions of temperature and O_2, the Fast

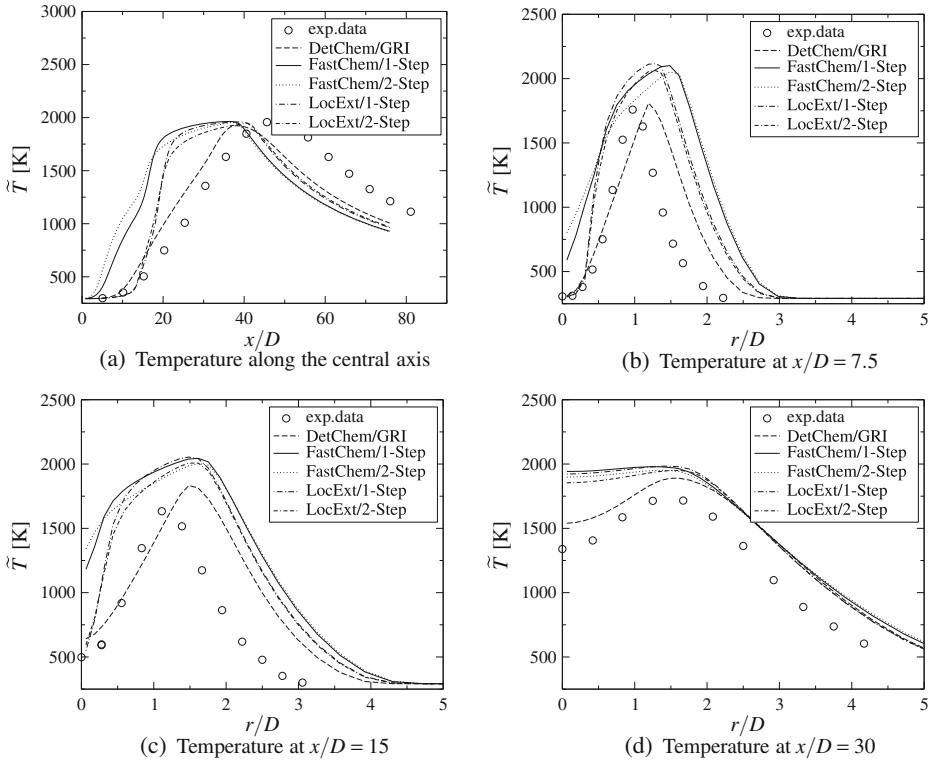

(a) Temperature along the central axis

(b) Temperature at $x/D = 7.5$

(c) Temperature at $x/D = 15$

(d) Temperature at $x/D = 30$

Fig. 3 Temperature predictions and measurements for the Flame D burner. Experimental data from Barlow and Frank [2] and simulations with the EDC and different approaches for the chemical kinetics. DetChem: Detailed Chemistry approach. FastChem: Fast Chemistry approach. LocExt: Local Extinction approach

Chemistry and Local Extinction approaches were very similar, overpredicting the temperature, and consuming all of the O_2 for r/D between 0 and 1. The Local Extinction approach with the two-step reaction predicted the lowest consumption of CH_4, whereas the Fast Chemistry approach, with the two-step reaction, predicted the highest consumption. The other approaches were in between these two. CO_2 was overpredicted with the Fast Chemistry and Local Extinction approaches and the one-step reaction, while using the two-step reaction, gave predictions similar to the Detailed Chemistry approach. This was also visible in the predictions of CO.

At $x/D = 45$ most of the CH_4 was consumed. The three main approaches gave closely the same predictions, and the levels of CO were close to zero.

In the initial phase of the study, Flame D was simulated with the fuel tube of the burner included in the domain. This was done in order to capture the development of the pipe flow prior to ejection into the open space of the flame. In these simulations, using the Fast Chemistry approach, the premixed rich fuel-air mixture burned inside the inlet pipe, consuming all the oxygen. This led to a large overprediction of the temperature in and close to the nozzle. However, using the Local Extinction or Detailed Chemistry approaches did not give notable major

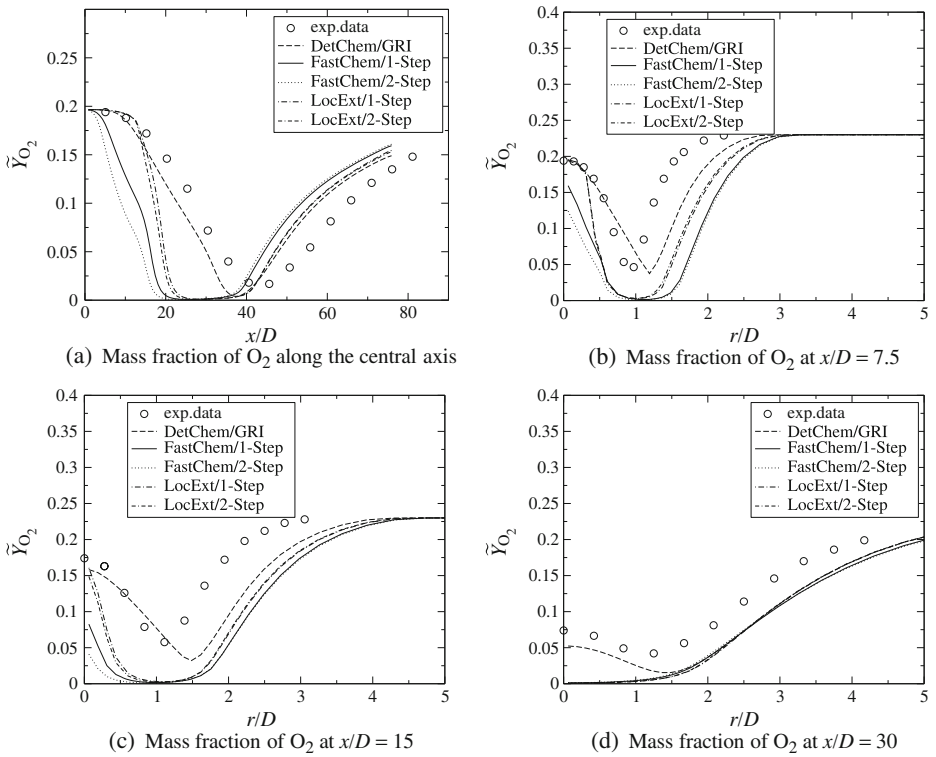

(a) Mass fraction of O_2 along the central axis

(b) Mass fraction of O_2 at $x/D = 7.5$

(c) Mass fraction of O_2 at $x/D = 15$

(d) Mass fraction of O_2 at $x/D = 30$

Fig. 4 O_2 mass-fraction predictions and measurements for the Flame D burner. Experimental data from Barlow and Frank [2] and simulations with the EDC and different approaches for the chemical kinetics. DetChem: Detailed Chemistry approach. FastChem: Fast Chemistry approach. LocExt: Local Extinction approach

reactions and temperature rise in the tube, and the nozzle-outlet temperature was not affected. The latter was in accordance with the experimental data.

Simulations of Flame E were performed with the turbulence-model constant $C_{\varepsilon 1}$ set to 1.60 (also 1.44 with the Local Extinction approach). Figure 7 shows the temperature profiles along the central axis. Flame E had more local extinction compared to Flame D. The experimental data for Flame E showed flame lift-off with centerline ignition at $x/D = 15$. Results from simulations of Flame E, with the three approaches for EDC, showed that the Fast Chemistry approach predicted ignition close to the jet nozzle (as in Flame D), whereas the Local Extinction and Detailed Chemistry approaches predicted centerline ignition at $x/D = 15$ and $x/D = 20$, respectively, and supressed the reactions in the mixing layer near the nozzle. The Detailed Chemistry approach predicted a lower temperature gradient along the central axis, compared to the Local Extinction approach. The results showed the ability of the Local Extinction approach to slow down the reactions and to allow the mixture to ignite further downstream. With $C_{\varepsilon 1} = 1.44$ and Local Extinction, the centerline temperature rise was moved approximately $1D$ upstream and made steeper from approximately $x/D = 22$, compared with the results shown. Also the centerline temperature peak was shifted towards the nozzle with a reduced $C_{\varepsilon 1}$.

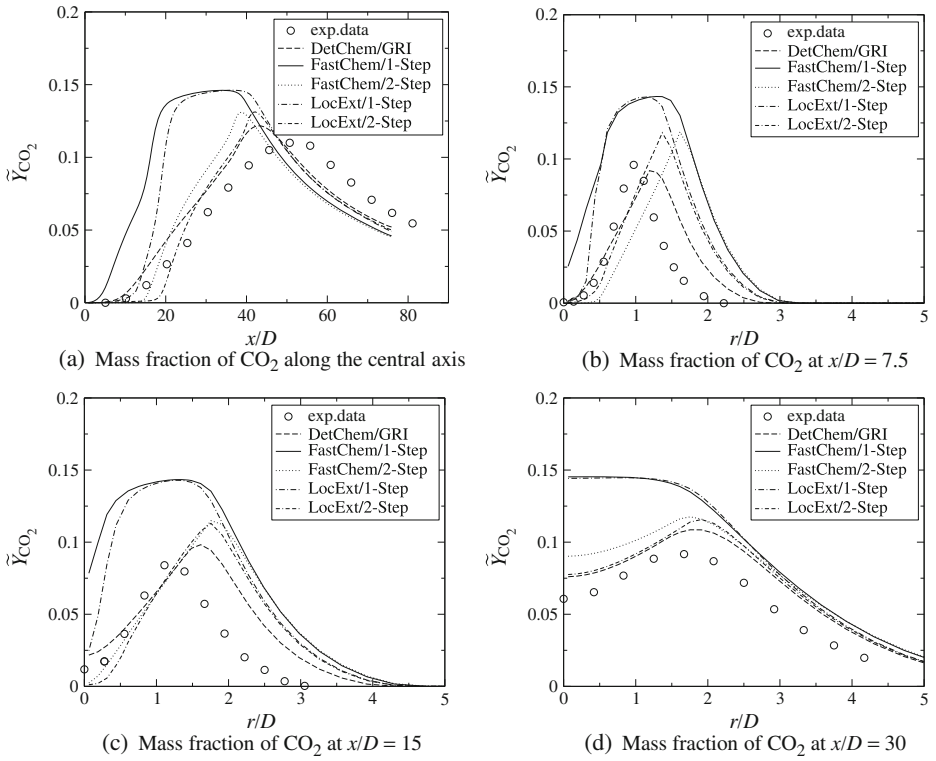

(a) Mass fraction of CO_2 along the central axis

(b) Mass fraction of CO_2 at $x/D = 7.5$

(c) Mass fraction of CO_2 at $x/D = 15$

(d) Mass fraction of CO_2 at $x/D = 30$

Fig. 5 CO_2 mass-fraction predictions and measurements for the Flame D burner. Experimental data from Barlow and Frank [2] and simulations with the EDC and different approaches for the chemical kinetics. DetChem: Detailed Chemistry approach. FastChem: Fast Chemistry approach. LocExt: Local Extinction approach

4.2 Piloted Premixed Jet Burner

Predictions of mean and RMS velocities for the Piloted Premixed Jet Burner (PPJB) compared to measurements from Dunn et al. [9, 10] showed small differences between the EDC approaches. Slight overpredictions of the mean velocities were observed. The calculated RMS velocities showed overpredictions compared to the measurements at the axial positions x/D equal to 5, 15 and 25. At $x/D = 35$ the RMS velocities were smaller than the measured values. The Fast Chemistry and Local Extinction approaches, predicted the highest RMS velocities at all positions, and thus predicted most mixing. The mean velocities resulting from the Fast Chemistry and Local Extinction calculations were larger than the mean velocities from the Detailed Chemistry approach at $x/D = 5$ and $x/D = 15$. At $x/D = 25$, the various EDC approaches predicted almost the same mean velocities, whereas at $x/D = 35$, the Detailed Chemistry approach predicted the highest mean velocities.

Figures 8, 9, 10, 11, 12 and 13 show predictions of temperatures, jet mixture fractions as well as mass fractions of O_2, CO_2, CH_4 and CO in the PPJB. The simulations are compared to experimental data from Dunn et al. [9, 10]. In general, the Detailed Chemistry approach gave the best predictions of the mean reaction rates

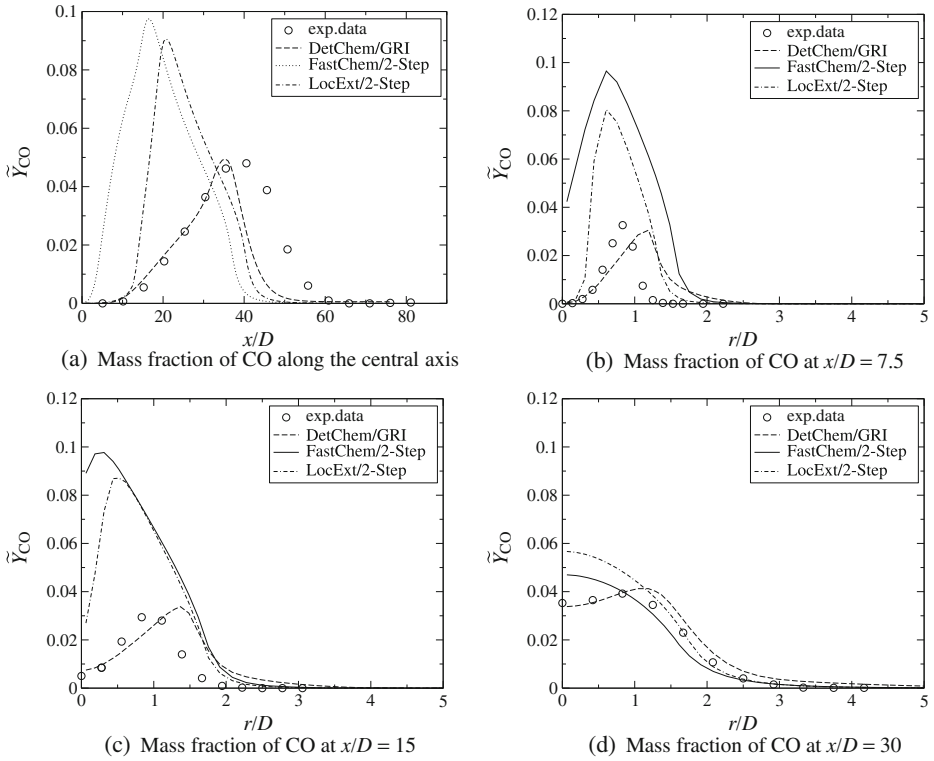

(a) Mass fraction of CO along the central axis
(b) Mass fraction of CO at $x/D = 7.5$
(c) Mass fraction of CO at $x/D = 15$
(d) Mass fraction of CO at $x/D = 30$

Fig. 6 CO mass-fraction predictions and measurements for the Flame D burner. Experimental data from Barlow and Frank [2] and simulations with the EDC and different approaches for the chemical kinetics. DetChem: Detailed Chemistry approach. FastChem: Fast Chemistry approach. LocExt: Local Extinction approach

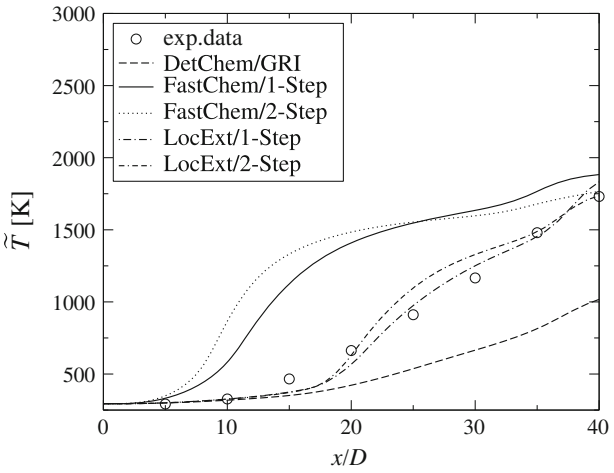

Fig. 7 Temperature predictions and measurements along the central axis for the Flame E burner. Experimental data from Barlow and Frank [2] and simulations with the EDC and different approaches for the chemical kinetics. DetChem: Detailed Chemistry approach. FastChem: Fast Chemistry approach. LocExt: Local Extinction approach

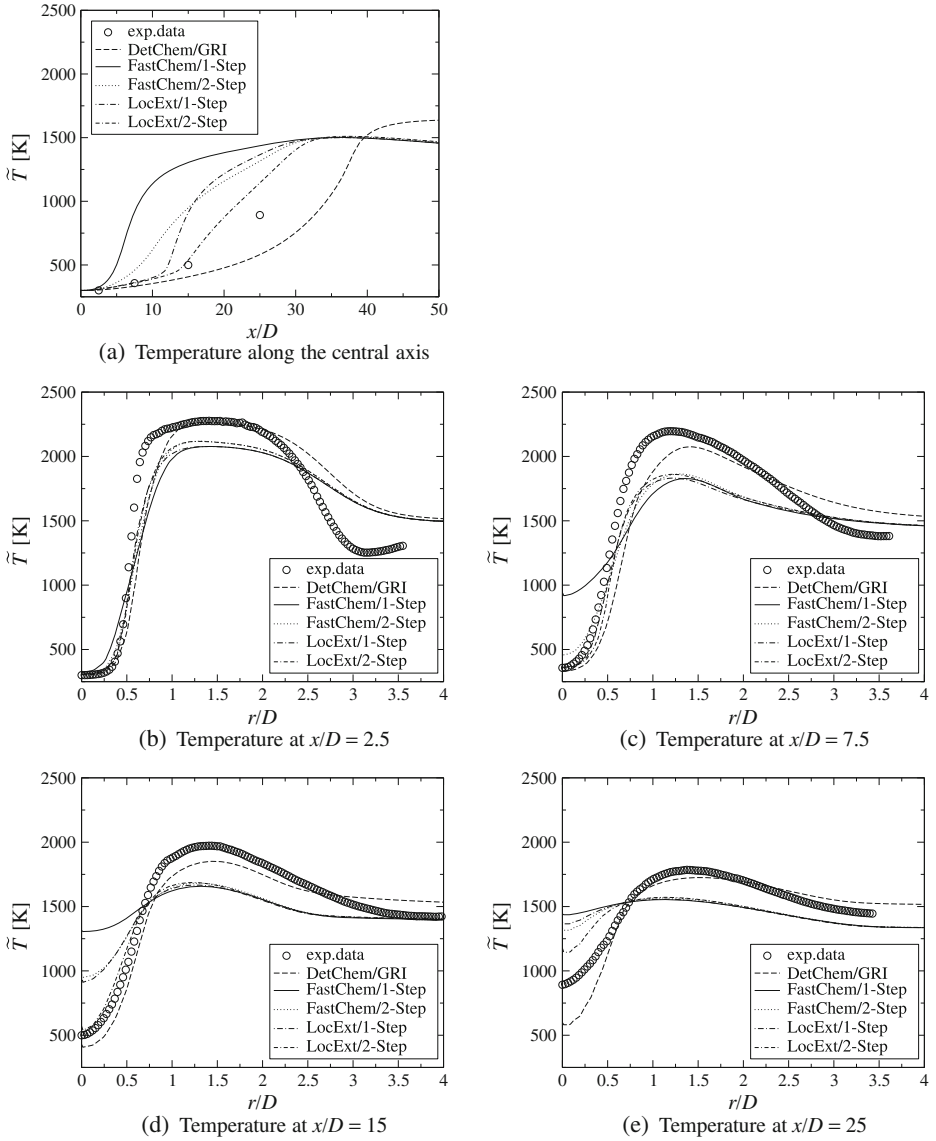

(a) Temperature along the central axis

(b) Temperature at $x/D = 2.5$

(c) Temperature at $x/D = 7.5$

(d) Temperature at $x/D = 15$

(e) Temperature at $x/D = 25$

Fig. 8 Temperature predictions and measurements for the PPJB. Experimental data from Dunn et al. [9, 10] and simulations with the EDC and different approaches for the chemical kinetics. DetChem: Detailed Chemistry approach. FastChem: Fast Chemistry approach. LocExt: Local Extinction approach

compared to the Fast Chemistry and Local Extinction approach. At the axial position $x/D = 2.5$, there were some minor differences between the three approaches. The Detailed Chemistry approach gave good predictions of temperature (Fig. 8b), whereas the other approaches underpredicted it. The jet mixture fraction (Fig. 9a) was the highest for the Fast Chemistry approach with the one-step reaction and

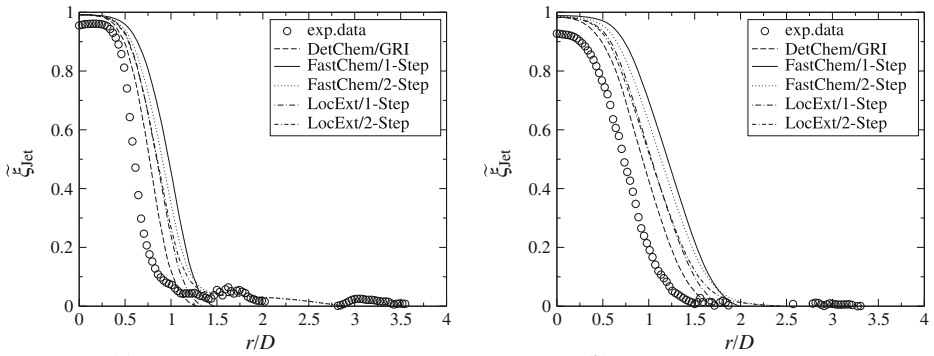

(a) Jet mixture fraction at $x/D = 2.5$ (b) Jet mixture fraction at $x/D = 7.5$

Fig. 9 Jet mixture-fraction predictions and measurements for the PPJB. Experimental data from Dunn et al. [9, 10] and simulations with the EDC and different approaches for the chemical kinetics. DetChem: Detailed Chemistry approach. FastChem: Fast Chemistry approach. LocExt: Local Extinction approach

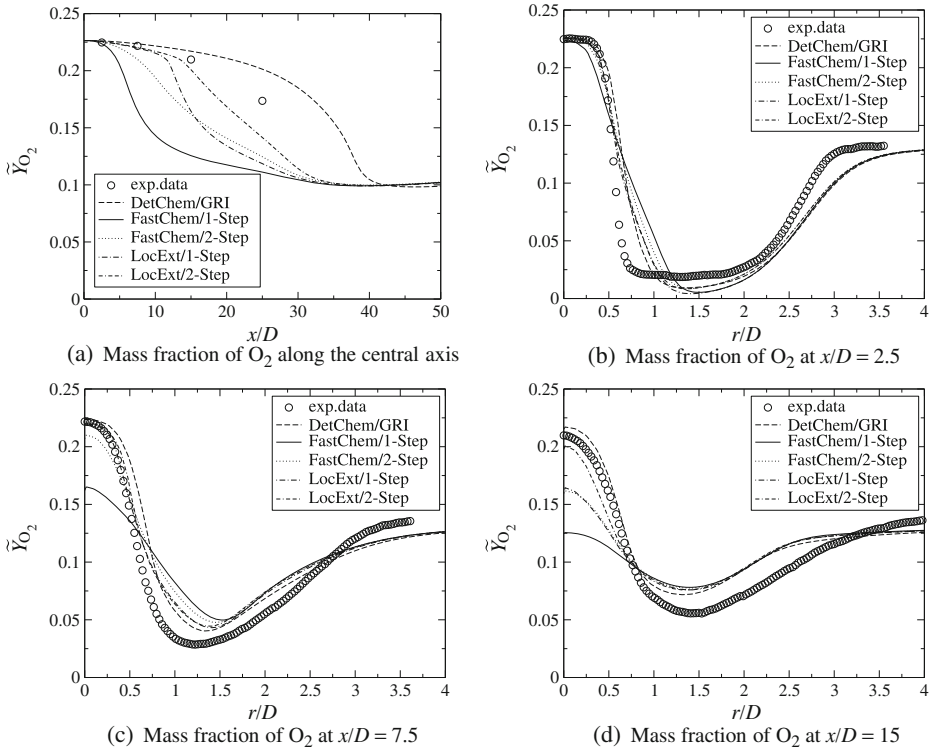

(a) Mass fraction of O_2 along the central axis (b) Mass fraction of O_2 at $x/D = 2.5$

(c) Mass fraction of O_2 at $x/D = 7.5$ (d) Mass fraction of O_2 at $x/D = 15$

Fig. 10 O_2 mass-fraction predictions and measurements for the PPJB. Experimental data from Dunn et al. [9, 10] and simulations with the EDC and different approaches for the chemical kinetics. DetChem: Detailed Chemistry approach. FastChem: Fast Chemistry approach. LocExt: Local Extinction approach

the Detailed Chemistry approach predicted the lowest values. The Fast Chemistry approach with the two-step reaction gave the second highest jet mixture fraction (Fig. 9a). The Local Extinction approach is very close to the Detailed Chemistry approach. This can also be seen in the plots of O_2 and CO_2 mass fractions, Figs. 10b and 11b. The one-step Fast Chemistry approach had the highest consumption of O_2 (and CH_4) and hence, the highest production of CO_2 and H_2O. The peak value of the CO mass fraction (Fig. 13a) was well predicted with the Detailed Chemistry approach, whereas the Fast Chemistry and the Local Extinction approach with the two-step reaction gave the same low values. The predictions of the coflow mixture fraction showed negligible differences between the three approaches for the axial positions studied.

At the axial position $x/D = 7.5$ the jet mixture fraction (Fig. 9b) showed the same distribution for the different approaches as for $x/D = 2.5$. The differences between the approaches became clearer at $x/D = 7.5$ compared to $x/D = 2.5$, especially at the radial positions r/D from 0 to 0.5. The one-step Fast Chemistry approach gave large overpredictions of the mean reaction rates in this area. This resulted in an overprediction of the temperature (Fig. 8c) in this region. Among the Fast

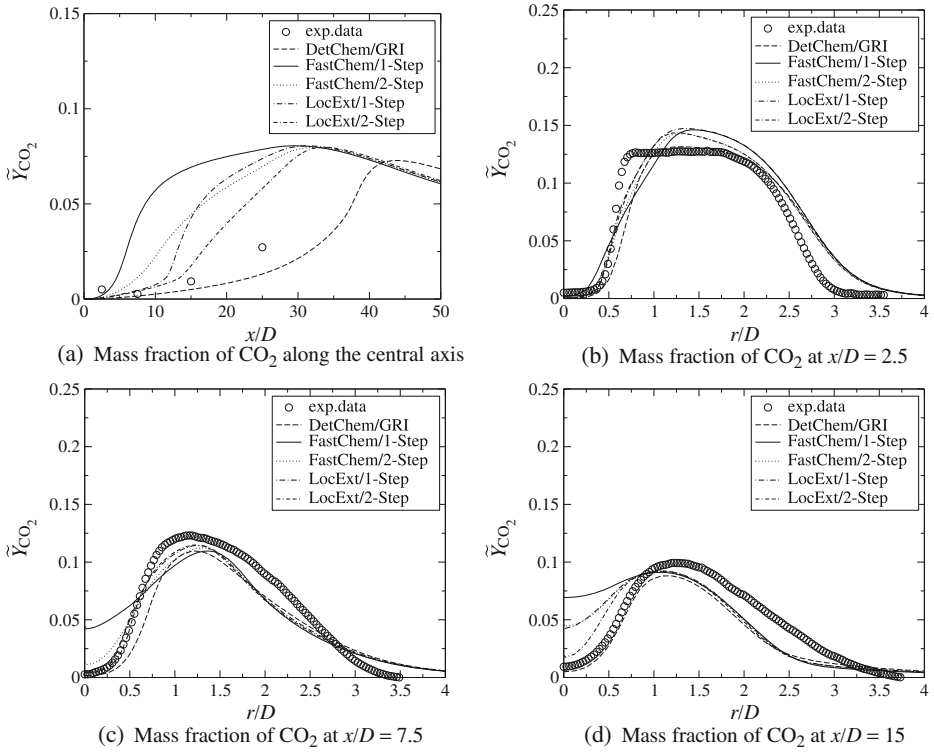

(a) Mass fraction of CO_2 along the central axis

(b) Mass fraction of CO_2 at $x/D = 2.5$

(c) Mass fraction of CO_2 at $x/D = 7.5$

(d) Mass fraction of CO_2 at $x/D = 15$

Fig. 11 CO_2 mass-fraction predictions and measurements for the PPJB. Experimental data from Dunn et al. [9, 10] and simulations with the EDC and different approaches for the chemical kinetics. DetChem: Detailed Chemistry approach. FastChem: Fast Chemistry approach. LocExt: Local Extinction approach

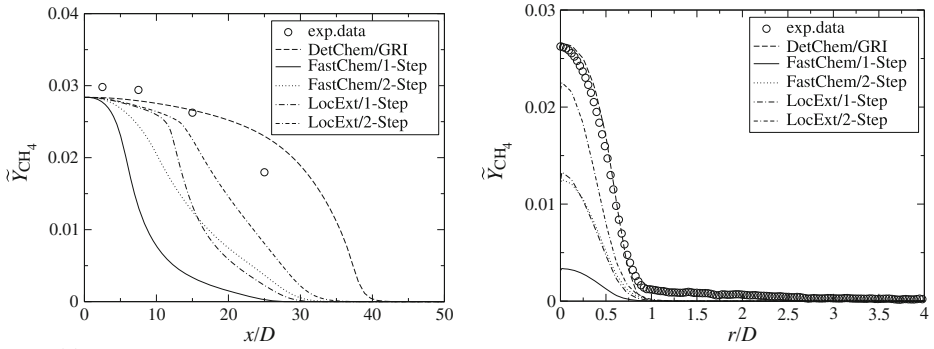

(a) Mass fraction of CH_4 along the central axis (b) Mass fraction of CH_4 at $x/D = 15$

Fig. 12 CH_4 mass-fraction predictions and measurements for the PPJB. Experimental data from Dunn et al. [9, 10] and simulations with the EDC and different approaches for the chemical kinetics. DetChem: Detailed Chemistry approach. FastChem: Fast Chemistry approach. LocExt: Local Extinction approach

Chemistry results, the two-step reaction apparently reduced the overall reaction rate. Apart from the Detailed Chemistry approach, the Local Extinction approach gave predictions closest to the measurements. In general, the Fast Chemistry and the Local Extinction approaches underpredicted the temperature at the radial positions between $r/D = 0.5$ and $r/D = 3$. The CO mass fractions (Fig. 13b) were fairly well predicted with Detailed Chemistry, with a peak value close to matching the measurements, however slightly shifted outwards compared to the measurements. The two-step Fast Chemistry and Local Extinction approaches, predicted levels of CO close to zero.

At the two axial positions further downstream, $x/D = 15$ and $x/D = 25$, the predictions of the jet mixture fractions were very similar for all EDC approaches. At $x/D = 15$, the trends among the different approaches were the same as for the

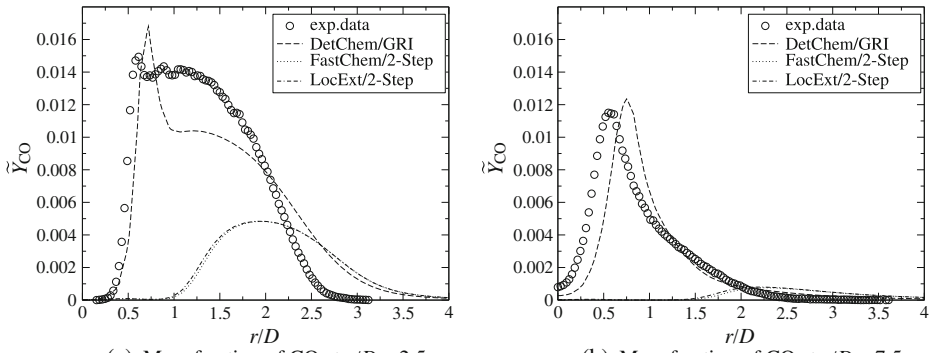

(a) Mass fraction of CO at $x/D = 2.5$ (b) Mass fraction of CO at $x/D = 7.5$

Fig. 13 CO mass-fraction predictions and measurements for the PPJB. Experimental data from Dunn et al. [9, 10] and simulations with the EDC and different approaches for the chemical kinetics. DetChem: Detailed Chemistry approach. FastChem: Fast Chemistry approach. LocExt: Local Extinction approach.

upstream positions, with the one-step Fast Chemistry approach giving the highest predictions of the mean reaction rates. For the temperature and major species, the two-step Fast Chemistry approach and the one-step Local Extinction approach gave nearly the same predictions at $x/D = 15$. The temperature profiles were seen (Fig. 8d) to be overpredicted at the radial positions from r/D equal 0 to 0.5. At $x/D = 15$, the Local Extinction approach with the two-step reaction gave predictions closest to both the Detailed Chemistry approach and the measurements at the radial positions from r/D equal 0 to 0.5. At $x/D = 15$ and $x/D = 25$ the Fast Chemistry and the Local Extinction approaches both underpredicted the temperatures, see Fig. 8, at the radial positions from r/D equal 0.5 to 3. At $x/D = 25$, predictions based on the Fast Chemistry and Local Extinction approaches were more similar, but the Local Extinction approach with the two-step reaction gave the best predictions. While the Fast Chemistry and the Local Extinction approach overpredicted reaction rates, the Detailed Chemistry approach showed underpredictions. The mass fraction of CO was fairly well predicted with the Detailed Chemistry approach, but for the Fast Chemistry and the Local Extinction approach, the levels were zero.

The profiles for the CH_4 mass fractions showed the Local Extinction approach slowing down the consumption of fuel also in the flame brush.

5 Discussion

Figures 2–13 show predicted results for a partially-premixed and a premixed jet flame, with three approaches for the inclusion of chemistry in the Eddy Dissipation Concept (EDC) for turbulent combustion. The Detailed Chemistry approach showed the best agreement with experimental data for both flames. Some of the discrepancies between the experimental data and predicted results for the premixed flame, especially for the Detailed Chemistry approach, can be attributed to uncertainties in the boundary conditions for the species in the pilot and coflow which is assumed to be in chemical equilibrium. The investigation of the exact mixture composition at the boundaries is still work in progress [4].

Merci and Dick [31] found that the choice of numerical discretization schemes was important for the spreading of the jet of Flame D. Moreover, they found that the applied combustion model and chemical kinetics model affected the spreading and mixing. In the present study, numerical schemes with second-order accuracy were applied and all cases were calculated as steady-state. Also, for the numerical grids applied, grid-convergence studies were performed. This indicated that the numerical discretization errors were small enough to allow the underlying mathematical models to be evaluated. In accordance with the findings of Merci and Dick [31], the predictions in this study also showed how the different approaches of the applied combustion model affected the spreading of the jet. In this study, grid convergence was investigated with the computationally fast approaches, which is a normal procedure when using the EDC. Performing such grid convergence studies by detailed chemistry calculations would be very computationally expensive. The minor species predicted in the detailed-chemistry calculations, such as OH, showed (relative) gradients and spikes comparable to those of the major species (e.g. H_2 and CO). This indicated that the grid convergence for the Fast Chemistry models could be representative for the Detailed Chemistry as well.

In the Flame D simulations, see Figs. 2–6, the Detailed Chemistry approach predicted peak values for scalars which are in acceptable agreement with the measurements, but shifted radially outwards compared to the measurements. The sharp temperature peak in the mixing layer near the burner outlet, which can be seen at $x/D = 7.5$ in both experiments and calculations with Detailed Chemistry, illustrates this shift most clearly. The temperature rise was predicted farther downstream with $C_{\varepsilon 1} = 1.60$ compared to $C_{\varepsilon 1} = 1.44$, due to weaker turbulent mixing and the associated delay of fuel conversion. Also the results for the PPJB, see Figs. 8–13, show that the spreading of the jet was overpredicted at some positions, even with the modified constant $C_{\varepsilon 1}$. As reported by Dunn et al. [11], the predictive capabilities of the RANS turbulence models were one of the contributors to mismatch between predictions and experimental data for the PPJB. In general a change in the value of $C_{\varepsilon 1}$ will result in good predictions in some positions and less good in other. This is why Launder and Spalding [24] suggested sliding (reduced downstream) values for $C_{\varepsilon 2}$ and C_{μ} for axisymmetric jets. It should also be noted from the literature reviewed in the Introduction that the choice of the detailed chemical reaction mechanism, used in the Detailed Chemistry approach, affects the prediction of the peak values and peak positions of the scalars, especially minor species, such as CO and OH. In this study, the GRI-Mech 3.0 mechanism [40] was used. Choosing another chemical kinetic mechanism with the same level of detail would have given slightly different predictions for the Detailed Chemistry approach but minor differences for the major species and the temperature, cf. Zahirović et al. [44]. The differences in the axial and radial CO plots, for both the Flame D and the PPJB, were far larger when comparing the Fast Chemistry and Local Extinction approaches to the Detailed Chemistry approach than a different choice of a detailed chemical reaction mechanism would predict. Similar observations with good agreement for major species but with increased CO levels when using reduced chemical mechanisms were made in [32]. The overall predictions of the flames with the Detailed Chemistry approach were in very good agreement with the reported measurements. The chemical time scales for the Local Extinction approach also depend on the mechanism. The influences of other detailed chemical kinetic mechanisms on the calculated time scales were not investigated in this study.

The Fast Chemistry and the Local Extinction approach were used with one-step and two-step reactions. In the one-step reaction, fuel (CH_4) and oxidizer (O_2) are converted directly to products, CO_2 and H_2O, in a stoichiometric order. The minimum of fuel or oxidizer controls the irreversible reaction. The two-step reaction gives a direct route for the conversion of CH_4 and O_2 to H_2O. CO is being produced in the first step of the reaction instead of CO_2, cf. Eq. 22. For the second step in the reaction, cf. Eq. 23, additional O_2 is needed for the conversion of CO to CO_2. The influence of the choice of either the one-step or the two-step reaction, in the Fast Chemistry and Local Extinction approaches, can be seen in the radial plots of both the Flame D and PPJB results. In the Flame D results, almost all of the O_2 was consumed in the r/D-range between 0 and 1.5, cf. Fig. 4, and CO_2 and CO were overpredicted, cf. Figs. 5 and 6a. The explanation for this is that the fuel jet is a fuel-rich mixture of CH_4 and air. Hence, the mass fraction of O_2 will be the minimum of the CH_4 and O_2 mass fractions in the mixture and control the reaction in the Fast Chemistry and Local Extinction calculations. Consuming the majority of the O_2 in the first reaction step, little O_2 is left for the conversion of CO to CO_2 in the second step. When using the two-step global reaction, the oxygen within Flame D was

slightly faster consumed compared with the one-step reaction, while the temperature was lower. This effect was mainly visible in the first part of the Flame D predictions, cf. Figs. 3a–c and 4a–c. This relation corresponds to the fact that the heat release per mole of O_2 consumed is less in the first reaction of the two-step mechanism than in the second (346 kJ and 566 kJ, respectively, per mole of O_2), and that the second reaction is delayed as long as there is methane left. At $x/D = 30$, all the oxygen inside the flame was consumed, cf. Fig. 4d. In the predictions of the PPJB, the levels of CO, see Fig. 13, are close to zero. The reason for this is that the fuel-jet mixture is a lean-fuel mixture of CH_4 and air, making the mass fractions of CH_4 the minimum component in the one-step and the two-step reaction for the Fast Chemistry and the Local Extinction approach. In the PPJB, CO is created but then directly converted to CO_2 due to the excess of O_2.

The Fast Chemistry approach will, for all premixed flames, overpredict the reaction rates because of its model assumptions. In the Detailed Chemistry approach, for both premixed and non-premixed flames, however, the predicted reaction rate will be zero if the turbulent mixing is too strong compared to the timescale of the chemistry (ignition or blow-off in the perfectly stirred reactor). The aim of this work was to study the effect of adding a constraint on the Fast Chemistry approach, which was named the Local Extinction approach, after Byggstøyl and Magnussen [5]. The residence time in the fine structure, τ^*, was compared to pre-calculated chemical time scales, τ_{ch}. The Local Extinction approach was seen to slow down the reaction rates in the areas with low values of τ^*, especially in the region around the jet with high levels of turbulence, but also in the flame brush. However, in the areas with lower levels of turbulence dissipation, i.e. higher values for τ^*, the Fast Chemistry and Local Extinction approaches behaved more similarly due to little or no constraint on the reaction rate. In the Flame D and E simulations, the Local Extinction approach had the largest effect on dampening the reaction rates, with both the one-step and two-step reactions behaving similarly in the jet-flow region. Also the Fast Chemistry approach, with both the one-step and two-step reactions, behaved very similarly. The major differences were seen in the predictions of CO and CO_2, as mentioned. In the simulations of Flame E, the Local Extinction approach predicted the lift-off nearly in accordance with the Detailed Chemistry approach. In the PPJB, the Fast Chemistry approach, with a one-step reaction, gave large overpredictions of the reaction rate. The best predictions, apart from the Detailed Chemistry approach, were achieved with the two-step Local Extinction approach. The advantage with the Local Extinction approach was its ability to delay the ignition of the mixtures. The best predictions were achieved with the Detailed Chemistry approach, but the ignition of the mixture was also fairly well predicted with the Local Extinction approach. However, the Fast Chemistry and Local Extinction approaches are identical when there is no local extinction, and hence, the reaction rates were overpredicted. The overpredicted reaction rate by the Fast Chemistry approach may lead to unphysical predictions if pre-inlet pipes are included in the computational domain due to the nature of the model. This does not occur with the the Local Extinction approach, which makes this approach more generally applicable and which represents a major benefit of this approach. Reactions are slowed down.

The turbulent flow in both burners has been modeled with the standard $k - \varepsilon$ turbulence model [24]. This is a very economical way to treat turbulence, but with its many simplifications the turbulent mixing is not well predicted for many types of flow. With better modeling of the turbulence, better predictions could be achieved,

especially with the Detailed Chemistry approach. However, a more detailed description of the flow, e.g. by performing a Large Eddy Simulation (LES) and using a very detailed chemical mechanism, is computationally very expensive, cf. Cleary et al. [6]. The Local Extinction approach has shown to incorporate some effects of detailed chemistry with reasonable computational expense. This recommends the Local Extinction approach for computationally expensive cases such as LES or industry-scale applications, where so far, Fast Chemistry or comparable approaches are commonly used. Especially predictions of the combustion in modern gas turbines that feature combustion chambers with highly turbulent flow would benefit from the inclusion of chemical kinetics since the flames show local extinction behavior due to finite chemical kinetic rates.

6 Conclusion

The Eddy Dissipation Concept (EDC) for turbulent combustion has been studied with three different approaches for modeling chemical kinetics: The Fast Chemistry approach, the Local Extinction approach and the Detailed Chemistry approach. All three model variants have been applied to two piloted diffusion flames and a piloted lean-premixed flame, and their predictions have been compared to experimental data from the literature. This also demonstrated that the same model can be consistently applied for both diffusion and premixed combustion cases. The Fast Chemistry approach overpredicted the reaction rate, as expected, while calculations with detailed chemical kinetics yielded results that were close to experimental data within modeling error of the turbulence model. The Local Extinction approach reproduced the location of the ignition point as well as the location of maximum temperature equally well as the detailed chemical kinetics approach. The overall heat release occurred faster since the tabulated model only employed one or two-step global chemical reactions.

An advantage of the Local Extinction approach, in addition to the incorporation of chemical kinetic effects, is that the simulation time is comparable to that of the Fast Chemistry approach, and many orders of magnitude lower than the Detailed Chemistry approach. However, in the consideration of chemical processes which rely heavily on detailed chemical kinetics, such as simulation of the formation of nitrogen oxides (NOx), the only appropriate approach is the Detailed Chemistry approach.

The method for determining the Local Extinction database in a numerical manner, as presented in this paper, now provides the possibility to apply the Local Extinction approach with fuels other than methane and oxidizers other than air.

Acknowledgements This work received support from the Research Council of Norway under the YGGDRASIL program (D. Christ) and through the Gas Technology Center NTNU-SINTEF (B. Lilleberg). The authors would like to thank senior principal specialist Nils Inge Lilleheie at ComputIT, Trondheim, for contributing with ideas to this paper. We would also like to thank Dr. Matthew J. Dunn for contributing with the experimental data on the premixed burner. The Norwegian Notur project (National infrastructure for computational science in Norway) and the Njord-cluster support staff are also thanked for making these simulations possible.

References

1. Amani, E., Nobari, M.R.H.: An efficient PDF calculation of flame temperature and major species in turbulent non-premixed flames. Appl. Math. Model. **34**(8), 2223–2241 (2010)
2. Barlow, R.S., Frank, J.H.: Effects of turbulence on species mass fractions in methane/air jet flames. Proc. Combust. Inst. **27**, 1087–1095 (1998)
3. Barlow, R., Frank, J., Dreizler, A.: International workshop on measurement and computation of turbulent nonpremixed flames. Sandia/TUD piloted CH_4/air jet flames (2007). URL http://www.sandia.gov/TNF/DataArch/FlameD.html, http://www.sandia.gov/TNF/DataArch/FlameD/SandiaPilotDoc21.pdf. Last visited March 2011
4. Barlow, R., Chen, J.Y., Dreizler, A., Dunn, M.J., Frank, J.H., Gordon, R., Hochgreb, S., Janicka, J., Kempf, A., Knudsen, E.W., Kronenburg, A., Lindstedt, R.P., Masri, A.R., Pitsch, H., Pope, S.B., Richardson, E.S., Roekaerts, D. (eds.): Tenth International Workshop on Measurement and Computation of Turbulent (Non)Premixed Flames, pp. 98–155 (2010). URL http://www.sandia.gov/TNF/10thWorkshop/TNF10.html. Last visited March 2011
5. Byggstøyl, S., Magnussen, B.F.: A model for flame extinction in turbulent flow. In: Fourth International Symposium on Turbulent Shear Flows, pp. 10.32–10.38 (1983)
6. Cleary, M., Klimenko, A., Janicka, J., Pfitzner, M.: A sparse-Lagrangian multiple mapping conditioning model for turbulent diffusion flames. Prog. Energy Combust. Sci. **32**(1), 1499–1507 (2009)
7. Dally, B.B., Fletcher, D.F., Masri, A.R.: Flow and mixing fields of turbulent bluff-body jets and flames. Combust. Theory Model. **2**(2), 193–219 (1998)
8. Dryer, F.L., Glassman, I.: High-temperature oxydation of CO and CH_4. Proc. Combust. Inst. **14**, 987–1003 (1973)
9. Dunn, M.J., Masri, A.R., Bilger, R.W.: A new piloted premixed jet burner to study strong finite-rate chemistry effects. Combust. Flame **151**(1-2), 46–60 (2007)
10. Dunn, M.J., Masri, A.R., Bilger, R.W., Barlow, R.S., Wang, G.H.: The compositional structure of highly turbulent piloted premixed flames issuing into a hot coflow. Proc. Combust. Inst. **32**(2), 1779–1786 (2009)
11. Dunn, M.J., Masri, A.R., Bilger, R.W., Barlow, R.S.: Finite rate chemistry effects in highly sheared turbulent premixed flames. Flow Turbul. Combust. **85**(3–4, Sp. Iss. SI), 621–648 (2010)
12. Ertesvåg, I.S., Magnussen, B.F.: The eddy dissipation turbulence energy cascade model. Combust. Sci. Technol. **159**, 213–235 (2000)
13. Gran, I.R.: Mathematical modeling and numerical simulation of chemical kinetics in turbulent combustion. Dr. Ing. thesis no. 1994:49, The Norwegian Institute of Technology, University of Trondheim (1994)
14. Gran, I.R., Magnussen, B.F.: A numerical study of a bluff-body stabilized diffusion flame. Part 2. Influence of combustion modeling and finite-rate chemistry. Combust. Sci. Technol. **119**, 191–217 (1996)
15. Gran, I.R., Melaaen, M.C., Magnussen, B.F.: Numerical simulation of local extinction effects in turbulent combustor flows of methane and air. Proc. Combust. Inst. **25**, 1283–1291 (1994)
16. Gran, I.R., Ertesvåg, I.S., Magnussen, B.F.: Influence of turbulence modeling on predictions of turbulent combustion. AIAA J. **35**, 106–110 (1997)
17. Habibi, A., Merci, B., Roekaerts, D.: Turbulence radiation interaction in Reynolds-averaged Navier–Stokes simulations of nonpremixed piloted turbulent laboratory-scale flames. Combust. Flame **151**(1–2), 303–320 (2007)
18. Hairer, E., Wanner, G.: Solving ordinary differential equations II: stiff and differential-algebraic problems. In: Springer Series in Computational Mathematics, 2nd rev. edn. Springer, Berlin (1996)
19. Hairer, E., Wanner, G.: Radau5 (2002). URL http://www.unige.ch/~hairer/prog/stiff/radau5.f, http://pitagora.dm.uniba.it/~testset/solvers/radau5.php. Last visited March 2011
20. Haworth, D.: Progress in probability density function methods for turbulent reacting flows. Prog. Energy Combust. Sci. **36**(2), 168–259 (2010)
21. Jones, W.P., Whitelaw, J.H.: Calculation methods for reacting turbulent flow: a review. Combust. Flame **48**, 1–26 (1982)
22. Kim, J.P., Schnell, U., Scheffknecht, G.: Comparison of different global reaction mechanisms for mild combustion of natural gas. Combust. Sci. Technol. **180**(4), 565–592 (2008)

23. Kronenburg, A., Kostka, M.: Modeling extinction and reignition in turbulent flames. Combust. Flame **143**, 342–356 (2005)
24. Launder, B.E., Spalding, D.B.: The numerical computation of turbulent flows. Comput. Methods Appl. Mech. Eng. **3**(2), 269–289 (1974)
25. Lilleberg, B., Ertesvåg, I.S., Rian, K.E.: Modeling instabilities in lean premixed turbulent combustors using detailed chemical kinetics. Combust. Sci. Technol. **181**(9), 1107–1122 (2009)
26. Magnussen, B.F.: On the structure of turbulence and a generalized Eddy Dissipation Concept for chemical reaction in turbulent flow. In: 19th AIAA Aerospace Science Meeting, 12–15 January, St. Louis, MO (1981)
27. Magnussen, B.F.: Modeling of NOx and soot formation by the Eddy Dissipation Concept. In: 1st topic Oriented Technical Meeting, 17–19 October, Int. Flame Research Foundation, Amsterdam, Holland (1989)
28. Magnussen, B.F., Hjertager, B.H.: On mathematical modeling of turbulent combustion with special emphasis on soot formation and combustion. Proc. Combust. Inst. **16**, 719–729 (1976)
29. Magnussen, B.F., Lilleheie, N.I., Vembe, B.E., Lakså, B., Grimsmo, B., Lilleeng, L.A., Kleiveland, R., Rian, K.E., Olsen, R., Evanger, T.: Numerical computation of large scale fires and fire mitigation—from combustion science to industry application. In: Sixth International Seminar on Fire and Explosion Hazards, 11–16 April, Leeds, UK (2010)
30. Masri, A.R., Cao, R., Pope, S.B., Goldin, G.M.: PDF calculations of turbulent lifted flames of H_2/N_2 fuel issuing into a vitiated co-flow. Combust. Theory Model. **8**(1), 1–22 (2004)
31. Merci, B., Dick, E.: Influence of computational aspects on simulations of a turbulent jet diffusion flame. Int. J. Numer. Methods Heat Fluid Flow **13**(7), 887–898 (2003)
32. Mustata, R., Valiño, L., Jiménez, C., Jones, W., Bondi, S.: A probability density function Eulerian Monte Carlo field method for large eddy simulations: application to a turbulent piloted methane/air diffusion flame (Sandia D). Combust. Flame **145**(1–2), 88–104 (2006)
33. Myhrvold, T., Ertesvåg, I.S., Gran, I.R., Cabra, R., Chen, J.Y.: A numerical investigation of a lifted H_2/N_2 turbulent jet flame in a vitiated coflow. Combust. Sci. Technol. **178**(6), 1001–1030 (2006)
34. OpenFOAM: OpenSource CFD Toolbox (2011). URL http://www.openfoam.com. Last visited March 2011
35. Panjwani, B., Ertesvåg, I.S., Rian, K.E., Gruber, A.: Subgrid combustion modelling for large eddy simulation (LES) of turbulent combustion using Eddy Dissipation Concept (EDC). In: Fifth European Conference on Computational Fluid Dynamics (2010)
36. Rowinski, D.H., Pope, S.B.: PDF calculations of piloted premixed jet flames. Combust. Theory Model. **15**(2), 245–266 (2011)
37. Schneider, C., Dreizler, A., Janicka, J., Hassel, E.P.: Flow field measurements of stable and locally extinguishing hydrocarbon-fueled jet flames. Combust. Flame **135**, 185–190 (2003)
38. Siegel, R., Howell, J.: Thermal Radiation Heat Transfer, 4th edn. Taylor & Francis, New York (2002)
39. Smith, T.F., Shen, Z.F., Friedman, J.N.: Evaluation of coefficients for the weighted sum of gray gases model. J. Heat Transf. Trans. ASME **104**(4), 602–608 (1982)
40. Smith, G.P., Golden, D.M., Frenklach, M., Moriarty, N.W., Eiteneer, B., Goldenberg, M., Bowman, C.T., Hanson, R.K., Song, S., Gardiner, J.W.C., Lissianski, V.V., Qin, Z.: GRI-Mech 3.0 (1999). URL http://www.me.berkeley.edu/gri_mech/. Last visited March 2011
41. Wang, H., Pope, S.B.: Lagrangian investigation of local extinction, re-ignition and auto-ignition in turbulent flames. Combust. Theory Model. **12**(5), 857–882 (2008)
42. Wang, H., Pope, S.B.: Time averaging strategies in the finite-volume/particle hybrid algorithm for the joint PDF equation of turbulent reactive flows. Combust. Theory Model. **12**(3), 529–544 (2008)
43. Waterson, N.P., Deconinck, H.: Design principles for bounded higher-order convection schemes—a unified approach. J. Comput. Phys. **224**, 182–207 (2007)
44. Zahirović, S., Scharler, R., Kilpinen, P., Obernberger, I.: Validation of flow simulation and gas combustion sub-models for the CFD-based prediction of NOx formation in biomass grate furnaces. Combust. Theory Model. **15**(1), 61–87 (2011)